

## Recent Developments in Oxide Ion Conductors: Aurivillius Phases

Kurt R. Kendall, Carlos Navas, Julie K. Thomas, and Hans-Conrad zur Loye\*

Massachusetts Institute of Technology, Cambridge, Massachusetts 02139

Received July 10, 1995. Revised Manuscript Received November 7, 1995<sup>⊗</sup>

Recent advances in the study of Aurivillius phases ( $\text{Bi}_2\text{A}_{n-1}\text{B}_n\text{O}_{3n+3}$ ,  $n = 1-5$ ) as oxide ion conductors are presented. The structures of modified Aurivillius phases containing extrinsic oxygen vacancies as well as Aurivillius phases containing intrinsic oxygen vacancies are surveyed. A detailed discussion of the conductivity behavior of these Aurivillius phases is given.

### Introduction

Oxide ion conductors have been widely studied for use as components of fuel cells, oxygen sensors, oxygen pumps, and oxygen-permeable membrane catalysts.<sup>1-7</sup> In most of these applications high temperatures are required to achieve the relatively high oxygen fluxes required for efficient operation.<sup>8,9</sup> For example, solid oxide fuel cells (SOFCs) that utilize a yttria-stabilized zirconia (YSZ) electrolyte must be operated near 1000 °C.<sup>10</sup> There are many issues associated with the use of high operating temperatures, including the high cost of materials able to function at those temperatures, materials stability and compatibility, and the thermal degradation of the electrolyte itself. Decreasing the thickness of the solid electrolyte can increase the oxygen flux and thereby decrease the temperatures required to achieve a given flux; however, there are limitations to this approach.<sup>11</sup> It has, therefore, been desirable to develop new materials that exhibit high oxide ion conductivities at temperatures below 800 °C.

One such class of materials that has exhibited remarkably high oxide ion conductivity is based upon a layered bismuth oxide/perovskite structure first reported by Aurivillius in 1949 (Figure 1).<sup>12-14</sup> Aurivillius phases are generally formulated as  $\text{Bi}_2\text{A}_{n-1}\text{B}_n\text{O}_{3n+3}$  and consist of  $n$  perovskite-like layers ( $\text{A}_{n-1}\text{B}_n\text{O}_{3n+1}$ )<sup>2-</sup> sandwiched between bismuth–oxygen sheets ( $\text{Bi}_2\text{O}_2$ )<sup>2+</sup>.<sup>15-17</sup>

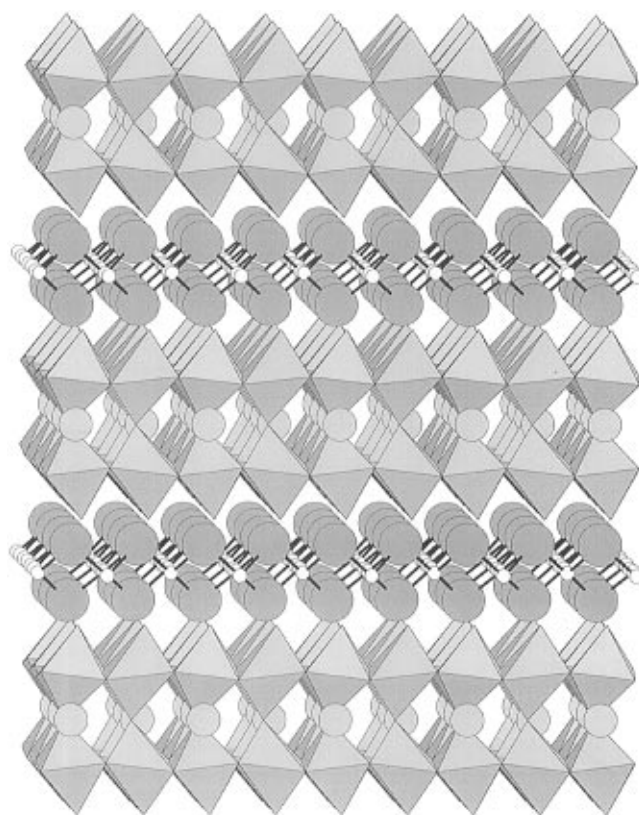


**Figure 1.**  $\text{Bi}_2\text{SrTa}_2\text{O}_9$ : Two octahedral “perovskite layers” separated by puckered bismuth oxide sheets. The octahedra consist of tantalum coordinated by six oxygens, while the large dark spheres represent bismuth, the large gray spheres represent strontium in a 12-coordinate site, and the small white spheres represent oxygen.

Aurivillius phases were originally of interest for their ferroelectric properties,<sup>18</sup> but in recent years, numerous researchers have explored the oxide ion conductivity of these phases. Table 1 lists some of the Aurivillius phases studied and their ionic conductivity. The materials examined to date fall into two classes: those containing intrinsic oxygen vacancies (e.g.,  $\text{Bi}_2\text{VO}_{5.5}$ ) and those with extrinsic oxygen vacancies (e.g.,  $\text{Bi}_2\text{Sr}_2\text{Nb}_2\text{-AlO}_{11.5}$ ) that are introduced by doping into either the

\* To whom correspondence should be addressed.

<sup>⊗</sup> Abstract published in *Advance ACS Abstracts*, January 15, 1996.

(1) Kudo, T.; Fueki, K. *Solid State Ionics*; VCH Publishers: New York, 1990.

(2) Steele, B. C. H. *Mater. Sci. Eng. B—Solid State Mater.* **1992**, *13*, 79.

(3) Minh, N. Q. *J. Am. Ceram. Soc.* **1993**, *76*, 563.

(4) Di Cosimo, R.; Burrington, J. D.; Grasselli, R. K. *J. Catal.* **1986**, *102*, 234.

(5) Cherrak, A.; Hubaut, R.; Barbaux, Y.; Mairesse, G. *Catal. Lett.* **1992**, *15*, 377.

(6) Barrault, J.; Grosset, C.; Dion, M.; Ganne, M.; Tournoux, M. *Catalysis Lett.* **1992**, *16*, 203.

(7) Harold, M. P.; Lee, C.; Burggraaf, A. J.; Keizer, K.; Zaspalis, V. T.; de Lange, R. S. A. *MRS Bull.* **1994**, April, 34.

(8) Dell, R. M.; Hooper, A. In *Solid Electrolytes*; Hagenmüller, P., van Gool, W., Ed.; Academic Press: New York, 1978; p 291.

(9) Riess, I. In *Science and Technology of Fast Ion Conductors*; Tuller, H. L., Balkanski, M., Ed.; Plenum Press: New York, 1987; p 23.

(10) Sammells, A. F.; Cook, R. L.; White, J. H.; Osborne, J. J.; MacDuff, R. C. *Solid State Ionics* **1992**, *52*, 111.

(11) Deng, H.; Zhou, M.; Abeles, B. *Solid State Ionics* **1994**, *74*, 75.

(12) Aurivillius, B. *Ark. Kemi.* **1949**, *1*, 463.

(13) Aurivillius, B. *Ark. Kemi.* **1949**, *1*, 499.

(14) Aurivillius, B. *Ark. Kemi.* **1949**, *2*, 519.

(15) Rae, A. D.; Thompson, J. G.; Withers, R. L. *Acta Crystallogr. B—Struct. Sci.* **1992**, *B48*, 418.

(16) Subbarao, E. C. *J. Am. Ceram. Soc.* **1962**, *45*, 166.

(17) Frit, B.; Mercurio, J. P. *J. Alloys Comp.* **1992**, *188*, 27.

(18) Subbarao, E. C. *J. Phys. Chem. Solids* **1962**, *23*, 665.

**Table 1. Conductivities of Selected Oxide Ion Conductors<sup>a</sup>**

compound	T (°C)	$\sigma$ (S/cm)	ref	notes
Bi <sub>4</sub> BaTi <sub>3</sub> ScO <sub>14.5</sub>	900	$2.5 \times 10^{-2}$	63	$n = 4$
Bi <sub>4</sub> BaTi <sub>3</sub> InO <sub>14.5</sub>	900	$4.9 \times 10^{-2}$	63	
Bi <sub>4</sub> BaTi <sub>3</sub> GaO <sub>14.5</sub>	900	$4.5 \times 10^{-2}$	63	
Bi <sub>2</sub> Sr <sub>2</sub> Nb <sub>2</sub> AlO <sub>11.5</sub>	800	$1.2 \times 10^{-2}$	64	$n = 3$
Bi <sub>2</sub> Sr <sub>2</sub> Nb <sub>2</sub> GaO <sub>11.5</sub>	800	$2.0 \times 10^{-2}$	64	
Bi <sub>2</sub> Sr <sub>2</sub> Ta <sub>2</sub> GaO <sub>11.5</sub>	800	$9.3 \times 10^{-3}$	64	
Bi <sub>2</sub> NaNbO <sub>8.5</sub>	900	$1 \times 10^{-2}$	60	$n = 2$
Bi <sub>2</sub> CaNb <sub>1.9</sub> Ti <sub>0.1</sub> O <sub>8.95</sub>	900	$5 \times 10^{-4}$	59	
Bi <sub>2</sub> WO <sub>6</sub>	900	$1 \times 10^{-2}$	26	$n = 1$
Bi <sub>2</sub> WO <sub>6</sub>	900	$1 \times 10^{-1}$	28	single crystal;    <i>ab</i> plane
Bi <sub>2</sub> VO <sub>5.5</sub>	300	$5 \times 10^{-5}$	52	$\alpha$ phase
	500	$1 \times 10^{-2}$	52	$\beta$ phase
	600	$1 \times 10^{-1}$	52	$\gamma$ phase
Bi <sub>2</sub> VO <sub>5.5</sub>	300	$1 \times 10^{-5}$	67	single crystal;    <i>ab</i> plane
	500	$1 \times 10^{-2}$	67	single crystal;    <i>ab</i> plane
	600	$3 \times 10^{-1}$	67	single crystal;    <i>ab</i> plane
Bi <sub>2</sub> VO <sub>5.5</sub>	300	$1 \times 10^{-6}$	67	single crystal; $\perp$ <i>ab</i> plane
	500	$1 \times 10^{-4}$	67	single crystal; $\perp$ <i>ab</i> plane
Bi <sub>2</sub> V <sub>0.9</sub> Cu <sub>0.1</sub> O <sub>5.35</sub>	300	$3.2 \times 10^{-3}$	55	
	500	$5 \times 10^{-2}$	52	
Bi <sub>2</sub> V <sub>0.9</sub> Co <sub>0.1</sub> O <sub>5.35</sub>	300	$6 \times 10^{-4}$	74	
	500	$7 \times 10^{-2}$	74	
Bi <sub>2</sub> V <sub>0.9</sub> Fe <sub>0.1</sub> O <sub>5.40</sub>	650	$6.7 \times 10^{-2}$	5	
Bi <sub>2</sub> V <sub>0.7</sub> Nb <sub>0.3</sub> O <sub>5.5</sub>	300	$1 \times 10^{-3}$	51	
	500	$5 \times 10^{-2}$	51	
Bi <sub>2</sub> V <sub>0.93</sub> Ni <sub>0.07</sub> O <sub>5.395</sub>	300	$1 \times 10^{-2}$	55	
	500	$1 \times 10^{-1}$	55	
Bi <sub>2</sub> V <sub>0.7</sub> Sb <sub>0.3</sub> O <sub>5.5</sub>	300	$1 \times 10^{-2}$	51	
	500	$1 \times 10^{-1}$	51	
Bi <sub>2</sub> V <sub>0.9</sub> Sr <sub>0.1</sub> O <sub>5.35</sub>	650	$1.2 \times 10^{-2}$	5	
Bi <sub>2</sub> V <sub>0.9</sub> Ti <sub>0.1</sub> O <sub>5.35</sub>	300	$1 \times 10^{-3}$	71	
	500	$5 \times 10^{-2}$	71	
Bi <sub>2</sub> V <sub>0.9</sub> Zn <sub>0.1</sub> O <sub>5.35</sub>	300	$1 \times 10^{-3}$	67	
	500	$5 \times 10^{-2}$	67	

<sup>a</sup> All conductivity data were measured using polycrystalline samples except where noted.

perovskite or the bismuth oxide layer. The metal-doped bismuth vanadium system (BIMEVOX) has some of the highest ionic conductivities reported. In this review we present a brief background on oxide ion conductors, followed by an examination of recent advances in the study of Aurivillius phases as oxide ion conductors. The structural aspects and a detailed description of their conductivity behavior is discussed.

### Background

In solid-state oxide ion conductors, vacancy hopping is the most common transport mechanism and, consequently, most materials studied contain oxygen vacancies.<sup>1</sup> The usual way to create extrinsic anion vacancies is through doping with aliovalent cations. Calcia- and yttria-stabilized zirconias (Ca<sub>x</sub>Zr<sub>1-x</sub>O<sub>2-x</sub> and Y<sub>x</sub>Zr<sub>1-x</sub>O<sub>2-0.5x</sub>) are examples of this type of doped-oxide material. A detailed description of the defect chemistry associated with dopants and its relationship to oxide ion conductivity has been recently published by Maier.<sup>19</sup>

In the past, systems that have been investigated included the stabilized zirconias and doped bismuth oxides. An Arrhenius plot of the conductivity for several oxide ion conductors is shown in Figure 2. Common to many of these oxygen-ion conductors is the fluorite structure, which ZrO<sub>2</sub> adopts at high temperatures. This cubic phase of ZrO<sub>2</sub> can be stabilized to lower temperatures by doping with aliovalent cations while simultaneously introducing oxygen vacancies. Doped cerium oxide and the high-temperature phase of bismuth oxide,

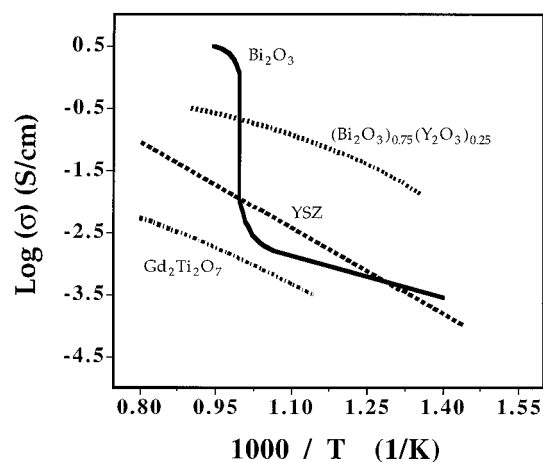


**Figure 2.** Arrhenius plot of conductivity for yttria-stabilized zirconia, YSZ,<sup>83</sup> bismuth oxide, Bi<sub>2</sub>O<sub>3</sub>,<sup>26</sup> yttria-stabilized bismuth oxide, (Bi<sub>2</sub>O<sub>3</sub>)<sub>0.75</sub>(Y<sub>2</sub>O<sub>3</sub>)<sub>0.25</sub>,<sup>84</sup> and the pyrochlore, Gd<sub>2</sub>Ti<sub>2</sub>O<sub>7</sub>.<sup>85</sup> The sharp transition in Bi<sub>2</sub>O<sub>3</sub> is due to a phase transition to the defect fluorite structure.

$\delta$ -Bi<sub>2</sub>O<sub>3</sub>, also form the fluorite structure and, like stabilized zirconia, display high oxide-ion conductivity.<sup>20-23</sup>

In contrast to the doped phases of CeO<sub>2</sub> and ZrO<sub>2</sub>, the high-temperature phase of bismuth oxide contains intrinsic oxygen vacancies. The structure of  $\delta$ -Bi<sub>2</sub>O<sub>3</sub> is similar to that of the fluorite structure with one-quarter of the anion sites vacant (i.e., BiO<sub>1.5</sub>(V<sub>0</sub>)<sub>0.5</sub>, V<sub>0</sub> = vacancy) and is formed at temperatures above 730 °C. These oxygen vacancies are disordered throughout the lattice, yielding a conductivity approximately 3 orders of magnitude higher than that of the low-temperature  $\alpha$ -phase. Dopants such as yttria, (Bi<sub>2</sub>O<sub>3</sub>)<sub>1-x</sub>(Y<sub>2</sub>O<sub>3</sub>)<sub>x</sub>, have been introduced into bismuth oxide to help stabilize the  $\delta$ -phase down to 25 °C. For  $x = 0.25$ , conductivities as high as  $1.3 \times 10^{-2}$  S/cm have been observed at 500 °C.<sup>24</sup> By comparison, the conductivity of YSZ at 500 °C is only  $5 \times 10^{-4}$  S/cm.<sup>20</sup>

A problem that occurs with bismuth oxide and with many of the other alternatives to stabilized zirconia is their easy reduction at low partial pressures of oxygen. At oxygen partial pressures near one atmosphere the transference number,  $t_i$ , of bismuth oxide and most of its solid solutions is close to unity; however, as the partial pressure decreases, Bi<sub>2</sub>O<sub>3</sub> is partially reduced and electronic conductivity starts to predominate.<sup>1</sup>

In addition to the fluorite structure, another related structure type that has been investigated recently for its oxide ion conductivity is the pyrochlore structure. This structure is related to the fluorite structure and has the general formula A<sub>2</sub>B<sub>2</sub>O<sub>7</sub> (e.g., Gd<sub>2</sub>Zr<sub>2</sub>O<sub>7</sub>).<sup>25</sup>

Because all of the above-mentioned systems require high temperatures to achieve useful oxide ion conductivities (see Figure 2) there is a great deal of interest in developing new materials that exhibit high oxide ion conductivity ( $10^{-1}$ – $10^{-2}$  S/cm) at lower temperatures

(20) Kudo, T.; Obayashi, H. *J. Electrochem. Soc.* **1976**, *123*, 415.

(21) Takahashi, T.; Esaka, T.; Iwahara, H. *J. Appl. Electrochem.* **1977**, *7*, 303.

(22) Takahashi, T.; Iwahara, H.; Nagaj, Y. *J. Appl. Electrochem.* **1972**, *2*, 97.

(23) Tuller, H. L.; Nowick, A. S. *J. Electrochem. Soc.* **1975**, *122*, 255.

(24) Takahashi, T.; Iwahara, H. *Mater. Res. Bull.* **1978**, *13*, 1447.

(25) Tuller, H. L.; Moon, P. K. *Mater. Sci. Eng. B—Solid State Mater.* **1988**, *1*, 171.

(19) Maier, J. *Angew. Chem., Int. Ed. Engl.* **1993**, *32*, 313.

(400–800 °C). In recent years, Aurivillius phases have constituted an important new class of oxide ion conductors. Oxide ion conductivity was first reported in Aurivillius phases during the 1970s by Takahashi<sup>26,27</sup> and Yanovskii.<sup>28</sup> Though they have no intrinsic oxygen vacancies, the  $n = 1$  member  $\text{Bi}_2\text{WO}_6$  and the structurally related  $\text{Bi}_2\text{MoO}_6$  both exhibit high oxide ion conduction. In fact, ionic conductivities as high as  $10^{-1}$  S/cm at 950 °C have been observed in single crystals of  $\text{Bi}_2\text{WO}_6$  measured parallel to the bismuth oxide plane, while conductivities in a direction perpendicular to the bismuth oxide plane are about 100 times lower.<sup>28</sup> The transference number for  $\text{Bi}_2\text{WO}_6$  is almost unity at high  $p(\text{O}_2)$ ; however, it decreases rapidly to about 0.3 below an oxygen partial pressure of  $10^{-3}$  atm.<sup>29</sup> Observed conductivity values for polycrystalline samples are somewhat lower ( $10^{-2}$  S/cm at 900 °C) but still show transference numbers close to unity in an air–oxygen concentration cell.<sup>26</sup>

### Structure

Aurivillius phases consist of an intergrowth between puckered bismuth oxide layers  $(\text{Bi}_2\text{O}_2)^{2+}$  and perovskite blocks  $(\text{A}_{n-1}\text{B}_n\text{O}_{3n+1})^{2-}$  which contain from  $n = 1$  to 5 octahedral layers (Figure 1).<sup>15,30,31</sup> The  $(\text{Bi}_2\text{O}_2)^{2+}$  sheets have basal edge-shared  $\text{BiO}_4$  groups with the bismuth occupying the apex of a square pyramid and the oxygens forming the basal plane. It is possible to replace the bismuth fully or in part with elements such as antimony, lead, and tellurium,<sup>32–35</sup> however, the synthesis of single-phase materials containing such substitutions is difficult and does not appear to benefit the ionic conductivity.<sup>36</sup> The A and B sites can handle a variety of cations (A = Na, K, Ca, Sr, Ba, Bi, etc.; B = Fe, Cr, Ti, Ga, Nb, V, Mo, W, etc.),<sup>17</sup> with the restriction that the perovskite layer and the bismuth oxide layer must match structurally.<sup>37</sup> To prevent mixed electronic/ionic conductivity, however, cation selection should be restricted to monovalent cations only.

The diversity in cations that the structure can accommodate proves important when trying to introduce oxygen vacancies by doping with aliovalent cations. For example, Thomas et al. substituted  $\text{In}^{3+}$  for  $\text{Ti}^{4+}$  in the four-layer  $\text{Bi}_4\text{BaTi}_4\text{O}_{15}$ , creating a new oxygen-deficient Aurivillius phase with the formula  $\text{Bi}_4\text{BaTi}_3\text{InO}_{14.5}$ .<sup>38</sup> The behavior of the ionic conductivity of this system, and many of the other Aurivillius phases with oxygen

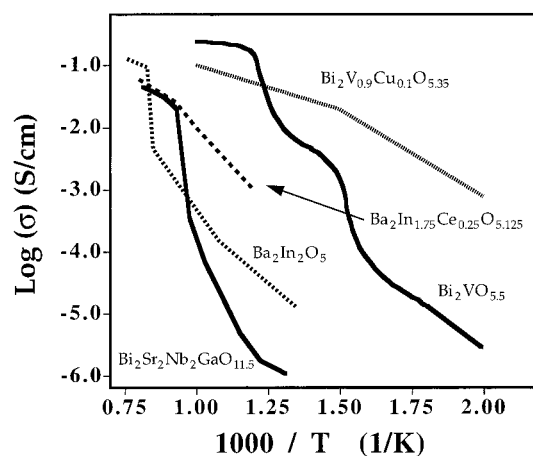


**Figure 3.** Arrhenius plot showing the conductivity of two brownmillerite/perovskite materials  $\text{Ba}_2\text{In}_2\text{O}_5$  and  $\text{Ba}_2\text{In}_{1.75}\text{Ce}_{0.25}\text{O}_{5.125}$ ,<sup>39</sup> along with  $\text{Bi}_2\text{VO}_{5.5}$ ,<sup>67</sup>  $\text{Bi}_2\text{V}_{0.9}\text{Cu}_{0.1}\text{O}_{5.35}$ ,<sup>52</sup> and  $\text{Bi}_2\text{Sr}_2\text{Nb}_2\text{GaO}_{11.5}$ .<sup>64</sup>

vacancies, is similar to that observed for the brownmillerite and perovskite structures.<sup>39,40</sup> For example, Figure 3 shows the ionic conductivity of two oxygen-deficient perovskites,  $\text{Ba}_2\text{In}_2\text{O}_5$  and  $\text{Ba}_2\text{In}_{1.75}\text{Ce}_{0.25}\text{O}_{5.125}$ , as well as several oxygen-deficient Aurivillius phases. The compounds with extrinsic oxygen vacancies all have similar ionic conductivities, while the ionic conductivities of Aurivillius phases with intrinsic oxygen vacancies are several orders of magnitude higher.

An Aurivillius phase that contains intrinsic as opposed to extrinsic oxygen vacancies is  $\text{Bi}_2\text{VO}_{5.5}$ . Discovered simultaneously and independently by Bush and Debreuille-Gresse,<sup>41,42</sup>  $\text{Bi}_2\text{VO}_{5.5}$  is a one-layer Aurivillius phase with intrinsic oxygen vacancies in the perovskite layer; the structure is shown in Figure 4.  $\text{Bi}_2\text{VO}_{5.5}$  undergoes two structural transitions to form three phases;  $\alpha$ ,  $\beta$ , and  $\gamma$ :<sup>43,44</sup>



These phase changes have been observed using differential thermal analysis (DTA) and differential scanning calorimetry (DSC), although a significant hysteresis is observed for the  $\alpha$ -to- $\beta$  transition on heating versus the  $\beta$ -to- $\alpha$  transition on cooling.<sup>43,45</sup> High-temperature X-ray diffraction experiments revealed that changes in crystallographic symmetry, from monoclinic for the  $\alpha$ -phase, to orthorhombic for the  $\beta$ -phase, to tetragonal for the  $\gamma$ -phase, accompanied the phase transitions.

More recently, Vannier et al. employed high-temperature X-ray diffraction of both powder and single

(26) Takahashi, T.; Iwahara, H. *J. Appl. Electrochem.* **1973**, *3*, 65.

(27) Takahashi, T.; Esaka, T.; Iwahara, H. *J. Appl. Electrochem.* **1977**, *7*, 31.

(28) Yanovskii, V. K.; Voronkova, V. I.; Roginskaya, Y. E.; Venevsev, Y. N. *Sov. Phys. Solid State Engl. Transl.* **1982**, *24*, 1603.

(29) Utkin, V. I.; Roginskaya, Y. E.; Voronkova, V. I.; Yanovskii, V. K. *Phys. Status Solidi A—Appl. Res.* **1980**, *59*, 75.

(30) Subbanna, G. N.; Guru Row, T. N.; Rao, C. N. R. *J. Solid State Chem.* **1990**, *86*, 206.

(31) Rae, A. D.; Thompson, J. G.; Withers, R. L. *Acta Crystallogr. B—Struct. Sci.* **1991**, *47*, 870.

(32) Castro, A.; Millan, P.; Martinez-Lope, M. J.; Torrance, J. B. *Solid State Ionics* **1993**, *63–65*, 897.

(33) Castro, A.; Millan, P.; Enjalbert, R.; Snoeck, E.; Galy, J. *Mater. Res. Bull.* **1994**, *29*, 871.

(34) Ramirez, A.; Millan, P.; Castro, A.; Torrance, J. B. *Eur. J. Solid State Inorg. Chem.* **1994**, *31*, 173.

(35) Millan, P.; Castro, A.; Torrance, J. B. *Mater. Res. Bull.* **1993**, *28*, 117.

(36) Vannier, R. N.; Mairesse, G.; Abraham, F.; Nowogrocki, G. *Solid State Ionics* **1994**, *70/71*, 248.

(37) Kikuchi, T. *Mater. Res. Bull.* **1979**, *14*, 1561.

(38) Thomas, J. K.; Anderson, M. E.; Krause, W. E.; zur Loye, H.-C., In *Materials Research Society Symposium Proceedings: Solid State Ionics*; Nazri, G.-A., Tarascon, J.-M., Armand, M., Ed.; MRS: Boston, MA, 1992; Vol. 293, p 295.

(39) Goodenough, J. B.; Ruiz-Diaz, J. E.; Zhen, Y. S. *Solid State Ionics* **1990**, *44*, 21.

(40) Kendall, K. R.; Navas, C.; Thomas, J. K.; zur Loye, H.-C. *Solid State Ionics* **1995**, *82*, 215.

(41) Bush, A. A.; Venetsev, Y. N. *Russ. J. Inorg. Chem.* **1986**, *31*, 769.

(42) Debreuille-Gresse, M.-F. Thesis, Universite de Lille, 1986.

(43) Abraham, F.; Debruelle-Gresse, M. F.; Mairesse, G.; Nowogrocki, G. *Solid State Ionics* **1988**, *28–30*, 529.

(44) Varma, K. B. R.; Subbanna, G. N.; Guru Row, T. N.; Rao, C. N. R. *J. Mater. Res.* **1990**, *5*, 2718.

(45) Lee, C. K.; Lim, G. S.; West, A. R. *J. Mater. Chem.* **1994**, *4*, 1441.

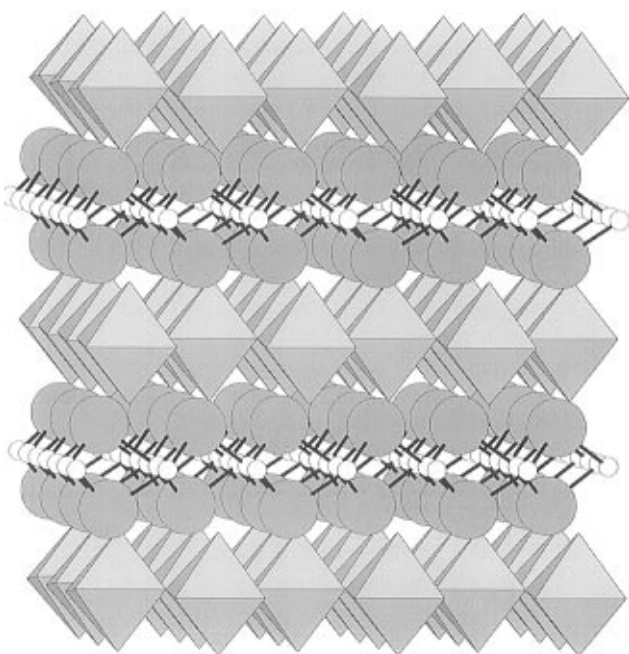


**Figure 4.** Structure of  $\text{Bi}_2\text{VO}_{5.5}$ . The space group and the atomic positions used to construct the picture were obtained from a single crystal structure reported by Touboul et al. in 1992.<sup>49</sup> The octahedra consist of vanadium coordinated to six oxygen/oxygen-vacancies. The large dark spheres represent bismuth, and the small white spheres represent oxygen.

crystals of  $\text{Bi}_2\text{VO}_{5.5}$ , along with differential scanning calorimetry (DSC) and impedance spectroscopy, to characterize in more detail the structure and the phase transitions;<sup>46</sup> the latter technique to correlate structural changes with oxide ion conductivity. The  $\alpha \rightleftharpoons \beta$  transition is associated with a complex structural transition from the  $\alpha$ -phase to the orthorhombic  $\beta$ -phase with a possible tetragonal intermediate phase. DSC results confirmed this complex behavior. The second phase transition from the  $\beta$ -phase to the  $\gamma$ -phase results in the tetragonal  $I4/mmm$  parent structure.

The high oxide ion conductivity exhibited by this material at elevated temperatures ( $>570^\circ\text{C}$ ) is believed to be due to disorder of the oxygen vacancies that are associated with the vanadium atoms in the perovskite layer. At lower temperatures, the oxygen vacancies are associated with the vanadium and form alternating vanadium-centered octahedra and tetrahedra.<sup>47</sup> At higher temperatures, the oxygen vacancies are disordered, with a concomitant increase in the conductivity.

There is some debate as to whether the  $\alpha$ -phase of  $\text{Bi}_2\text{VO}_{5.5}$  indeed has an Aurivillius structure. High-resolution electron microscopy (HREM) studies by Zhou did not show the characteristic  $(\text{Bi}_2\text{O}_2)^{2+}$  layer exhibited by  $\gamma$ - $\text{Bi}_2\text{MoO}_6$ .<sup>48</sup> Touboul solved the single-crystal structure of the low-temperature  $\alpha$ -phase and concluded that it was not a member of the Aurivillius family.<sup>49</sup> The structure was solved in the orthorhombic space group  $Aba2$  with lattice parameters  $a = 5.598(2) \text{ \AA}$ ,  $b = 15.292(9) \text{ \AA}$ , and  $c = 5.532(2) \text{ \AA}$ . According to these data

the bismuth bonds to three rather than four oxygens in the bismuth–oxygen layer, and the apical oxygen of the vanadium/oxygen octahedra bonds with the bismuth. This leads to distorted bismuth/oxygen tetrahedra in a  $(\text{Bi}_2\text{O}_{2.75})^{0.5+}$  layer. Vanadium forms a corner-sharing octahedral layer, as it would in an Aurivillius structure; however, the formula is best written as  $(\text{VO}_{2.75})^{0.5-}$ . The basis for this interpretation of the structure is the existence of an extremely short (1.89 Å) and an extremely long (2.74 Å) Bi–O bond in the  $(\text{Bi}_2\text{O}_2)^{2+}$  plane. The extremely short Bi–O bond of 1.89 Å, in conjunction with the absence of any reported superlattice reflections, however, tends to discourage the acceptance of this alternative structure.<sup>46</sup>

Using EXAFS, Francklin et al. examined a copper-doped system,  $\text{Bi}_2\text{V}_{0.95}\text{Cu}_{0.05}\text{O}_{5.425}$ , and reported results which were consistent with the crystal data reported by Touboul.<sup>50</sup> They did not, however, address the issue as to whether this material should be classified as an Aurivillius phase. The  $\text{Cu}^{2+}$  cations exchange for  $\text{V}^{5+}$  cations and lead to a slight increase in the metal/oxygen bond distances.

Joubert et al. performed a detailed Rietveld analysis with X-ray and neutron diffraction data on powdered samples of the  $\alpha$ - $\text{Bi}_2\text{VO}_{5.5}$  and concluded that it should be classified as an Aurivillius phase.<sup>47</sup> Furthermore, they performed electron diffraction experiments to elucidate the superstructure peaks observed in the diffraction data. Using X-ray, neutron, and electron diffraction data the structure was solved in the monoclinic space group  $C2/m$  with lattice parameters  $a = 5.6120(2) \text{ \AA}$ ,  $b = 15.2829(4) \text{ \AA}$ ,  $c = 16.6014(5) \text{ \AA}$ , and  $\beta = 89.756(1)^\circ$ . The structure consisted of alternating V–O tetrahedra and oxygen-deficient V–O octahedra with ordered oxygen vacancies along the monoclinic axis. Accordingly, they proposed a series of structural changes starting with ordered oxygen vacancies in the  $\alpha$ -phase, to nonequivalent vanadium–oxygen octahedra in the  $\beta$ -phase, to a more symmetrical structure for the  $\gamma$ -phase. Using powder X-ray diffraction with Rietveld refinement and HREM, Varma et al. also classified the  $\alpha$ -phase as an Aurivillius phase.<sup>44</sup>

Joubert et al. synthesized and solved the single-crystal structure for  $\text{Bi}_2\text{V}_{0.75}\text{Sb}_{0.25}\text{O}_{5.35}$ .<sup>51</sup> They classified this compound, which is orthorhombic, space group  $Fmmm$ , with lattice parameters  $a = 5.486(2) \text{ \AA}$ ,  $b = 5.513(2) \text{ \AA}$ , and  $c = 15.559(3) \text{ \AA}$ , as an Aurivillius phase. An XPS study on this material indicated that the vanadium is present in both the +4 and +5 oxidation state in the structure.

Abraham et al. solved the single-crystal structure of the high-temperature  $\gamma$ -phase in the space group  $I4/mmm$ . In the idealized tetragonal structure, the bismuth and vanadium occupy the 4e and 2b sites; however, splitting of the bismuth positions was required for adequate convergence.<sup>52</sup> Consequently, bismuth partially occupied the 16m and 4e site, while vanadium partially occupied the 8h site. These results imply that even the more symmetric high-temperature phase re-

(46) Vannier, R. N.; Mairesse, G.; Abraham, F.; Nowogrocki, G.; Pernot, E.; Anne, M.; Bacmann, M.; Strobel, P.; Fouletier, J. *Solid State Ionics* **1995**, *78*, 183.

(47) Joubert, O.; Jouanneaux, A.; Ganne, M. *Mater. Res. Bull.* **1994**, *29*, 175.

(48) Zhou, W. *J. Solid State Chem.* **1988**, *76*, 290.

(49) Touboul, M.; Lokaj, J.; Tessier, L.; Kettman, V.; Vrabel, V. *Acta Crystallogr. B-Struct. Sci.* **1992**, *C48*, 1176.

(50) Francklin, A. J.; Chadwick, A. V.; Couves, J. W. *Solid State Ionics* **1994**, *70/71*, 215.

(51) Joubert, O.; Jouanneaux, A.; Ganne, M.; Vannier, R. N.; Mairesse, G. *Solid State Ionics* **1992**, *73*, 309.

(52) Abraham, F.; Boivin, J. C.; Mairesse, G.; Nowogrocki, G. *Solid State Ionics* **1990**, *40/41*, 934.

**Table 2. Cation Dopant Concentration Required to Stabilize the Tetragonal Phase of Bi<sub>2</sub>VO<sub>5.5</sub>**

dopant cation	cation concentration <sup>a</sup>	ref
Li <sup>+</sup>	10%	86
Zn <sup>2+</sup>	10%	86
Pb <sup>2+</sup>	9% ≤ x ≤ 10%	78
Cu <sup>2+</sup>	7% < x < 12%	52, 56
Ni <sup>2+</sup>	10%	53, 71
Co <sup>2+</sup>	7.5% ≤ x ≤ 25%	74, 75
Sb <sup>5+</sup>	15% ≤ x ≤ 50%	51
Nb <sup>5+</sup>	10% ≤ x ≤ 50%	51, 71
Ta <sup>5+</sup>	10% ≤ x ≤ 25%	71
Ti <sup>4+</sup>	10% ≤ x ≤ 20%	71, 86
Zr <sup>4+</sup>	10% ≤ x ≤ 15%	71
Mg <sup>2+</sup>	7.5% ≤ x ≤ 15%	71

<sup>a</sup> Concentration is percent of vanadium substitution.

quires detailed analysis before the structure can be fully described.

Abraham et al., by substituting other metals (Me) into the vanadium site, succeeded in stabilizing the highly conductive  $\gamma$ -phase to lower temperatures, generating the BIMEVOX family of doped Bi-V oxides.<sup>52</sup> For example, if Cu<sup>2+</sup> is used as the dopant, the general formula would be Bi<sub>2</sub>V<sub>1-x</sub>Cu<sub>x</sub>O<sub>5.5-1.5x</sub>. For x = 0.1, i.e., BICUVOX.10, the stoichiometry would be Bi<sub>2</sub>V<sub>0.9</sub>Cu<sub>0.1</sub>O<sub>5.35</sub>. Studies of solid solutions containing various cation dopants have been carried out. Above a certain level of dopant, BIMEVOX compounds take on the structure of  $\gamma$ -Bi<sub>2</sub>VO<sub>5.5</sub>,<sup>53</sup> while below that doping level, compounds are typically isostructural with  $\alpha$ -Bi<sub>2</sub>VO<sub>5.5</sub>.

Aboukais et al. used EPR and UV-visible spectroscopy to characterize the copper and vanadium environments in BICUVOX.<sup>54</sup> The data were consistent with distorted oxygen octahedra around the copper, with a compression of the apical oxygen. In addition, they reported that the vanadium was present predominately as V<sup>5+</sup> rather than V<sup>4+</sup>.

There is some discrepancy in the literature concerning the required amount of a given dopant necessary to achieve the tetragonal  $\gamma$ -phase. For instance, Pernot et al. claimed that with 7% Cu doping the structure was tetragonal,<sup>55</sup> whereas Goodenough et al. and Lee et al. separately determined that a higher value (ca. 15%) was necessary.<sup>45,56</sup> Lee studied the ternary phase diagram of the Bi<sub>2</sub>O<sub>3</sub>-V<sub>2</sub>O<sub>5</sub>-MeO (Me = Co, Cu, Zn, Ca, and Sr) system for a number of metal cations and determined the minimum amount of dopant necessary to achieve the tetragonal structure. A compilation of several groups' findings for the minimum dopant concentrations required to stabilize the  $\gamma$ -phase is listed in Table 2.

One assumption concerning the doping process that has been called into question in these systems is that of exclusive doping into the directed site.<sup>36,45</sup> For example, it is usually assumed that the vanadium is replaced without disturbing the bismuth oxide layer. Lee et al. has examined this assumption,<sup>45,57</sup> and has suggested that in addition to Me  $\leftrightarrow$  V substitutions, Bi

(53) Anne, M.; Bacmann, M.; Pernot, E.; Abraham, F.; Mairesse, G.; Strobel, P. *Physica B* **1992**, *180*, 181, 621.

(54) Aboukais, A.; Delmaire, F.; Rigole, M.; Hubaut, R.; Mairesse, G. *Chem. Mater.* **1993**, *5*, 1819.

(55) Pernot, E.; Anne, M.; Bacmann, M.; Strobel, P.; Fouletier, J.; Vannier, R. N. Mairesse, G.; Abraham, F.; Nowogrocki, G. *Solid State Ionics* **1994**, *70/71*, 259.

(56) Goodenough, J. B.; Manthiram, A.; Parantham, M.; Zhen, Y. S. *Mater. Sci. Eng. B—Solid State Mater.* **1992**, *12*, 357.

(57) Lee, C. K.; Sinclair, D. C.; West, A. R. *Solid State Ionics* **1993**, *62*, 193.

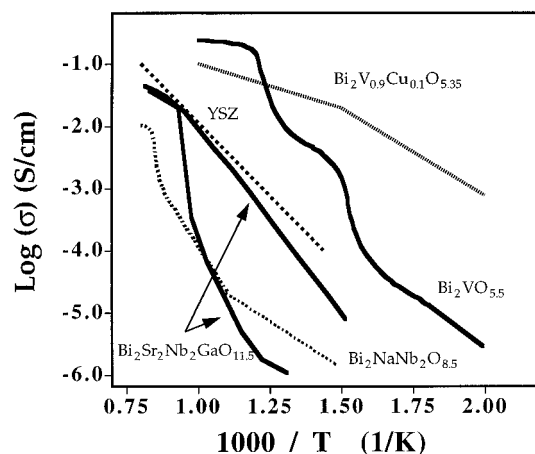


**Figure 5.** Arrhenius plot showing the conductivity of Bi<sub>2</sub>VO<sub>5.5</sub>,<sup>67</sup> Bi<sub>2</sub>V<sub>0.9</sub>Cu<sub>0.1</sub>O<sub>5.35</sub>,<sup>52</sup> YSZ,<sup>83</sup> Bi<sub>2</sub>Sr<sub>2</sub>Nb<sub>2</sub>GaO<sub>11.5</sub> heating (lower curve),<sup>64</sup> Bi<sub>2</sub>Sr<sub>2</sub>Nb<sub>2</sub>GaO<sub>11.5</sub> cooling (upper curve), and Bi<sub>2</sub>NaNb<sub>2</sub>O<sub>8.5</sub>.<sup>60</sup> With the exception of YSZ, all of the materials exhibit a discontinuity in their Arrhenius plots associated with an order/disorder phase transition. Bi<sub>2</sub>Sr<sub>2</sub>Nb<sub>2</sub>GaO<sub>11.5</sub> also shows severe hysteresis in its conductivity.

$\leftrightarrow$  V and Me  $\leftrightarrow$  Bi substitutions also take place. Furthermore, it was suggested that the dopant, Me, could occupy interstitial sites as well. Using phase diagrams for Bi<sub>2</sub>O<sub>3</sub>-V<sub>2</sub>O<sub>5</sub>-MeO (Me = Co, Cu, Zn, Ca, Sr),<sup>45</sup> it was demonstrated that, depending on the cation involved, any one of the three substitutions was possible, and in some cases required, if the compound was to form in the Bi<sub>2</sub>VO<sub>5.5</sub> structure.

An important aspect of the bismuth vanadium system is the range of compositions possible. Bi<sub>2</sub>VO<sub>5.5</sub> is in fact the upper limit for Bi<sub>2+x</sub>VO<sub>5.5</sub> (x = 1-1.16).<sup>46</sup> In addition to the work by Lee and co-workers, Lazure et al. recently addressed this concern for Bi<sub>2</sub>(V<sub>1-x-y</sub>Co<sub>x</sub>Bi<sub>y</sub>)O<sub>z</sub>.<sup>58</sup> A maximum cobalt doping (x = 0.25) was associated with a slight bismuth excess (y = 0.04), while the maximum bismuth excess (y = 0.06) was associated with a smaller cobalt doping concentration (x = 0.10). The bismuth is believed to replace the vanadium in the perovskite region. In no case is there indication of bismuth insertion into an interstitial site.

## Conductivity

**Substitutions in Perovskite Region.** Aliovalent substitutions in the A and B sites of the perovskitic region in Aurivillius phases, Bi<sub>2</sub>A<sub>n-1</sub>B<sub>n</sub>O<sub>3n+3</sub>, can lead to a significant enhancement of the ionic conductivity. Figure 5 contains Arrhenius plots for several Aurivillius systems. Jacobson and co-workers performed A and B site substitution on the two-layer phase Bi<sub>2</sub>CaNb<sub>2</sub>O<sub>9</sub>, to determine the relative importance of the two sites.<sup>59</sup> They substituted Na<sup>+</sup> for Ca<sup>2+</sup> on the A site and Ti<sup>4+</sup> for Nb<sup>5+</sup> on the B site. Solid solutions were obtained for Bi<sub>2</sub>Na<sub>x</sub>Ca<sub>1-x</sub>Nb<sub>2</sub>O<sub>9-x/2</sub>, 0 ≤ x ≤ 1, and Bi<sub>2</sub>Ca<sub>1</sub>Nb<sub>2-y</sub>Ti<sub>y</sub>O<sub>9-y/2</sub>, 0 ≤ y ≤ 0.15, creating new oxygen-deficient Aurivillius phases.<sup>60</sup>

The ionic conductivity of the A-site substituted Aurivillius phase, Bi<sub>2</sub>Na<sub>x</sub>Ca<sub>1-x</sub>Nb<sub>2</sub>O<sub>9-x/2</sub>, showed little

(58) Lazure, S.; Vannier, R. N.; Nowogrocki, G.; Mairesse, G.; Muller, C.; Anne, M.; Strobel, P. *J. Mater. Chem.* **1995**, *5*, 1395.

(59) Pham, A.-Q.; Yazdi, I.; Jacobson, A. J. *J. Electrochem. Soc.* **1995**, *142*, 1559.

(60) Pham, A.-Q.; Puri, M.; DiCarlo, J.; Jacobson, A. J. *Solid State Ionics* **1994**, *72*, 309.

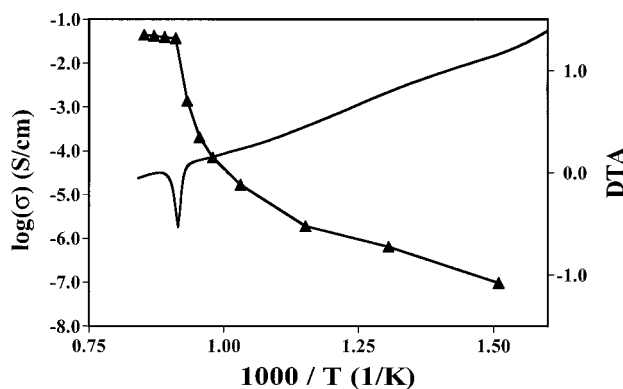


**Figure 6.** Arrhenius plot of conductivity and DTA data for  $\text{Bi}_4\text{BaTi}_3\text{GaO}_{14.5}$ . The discontinuity in the Arrhenius plot coincides with the endothermic transition in the DTA data.

change for  $x \leq 0.1$ ; however, for larger values of  $x$ , the conductivity increased by an order of magnitude. A discontinuity was observed in the Arrhenius plot at 860 °C and was attributed to an order/disorder phase transition. For  $\text{Bi}_2\text{NaNb}_2\text{O}_{8.5}$ , the conductivity was  $10^{-2}$  S/cm at 900 °C. This order/disorder transition appears in many of the Aurivillius phases with extrinsic oxygen vacancies and is similar to the transitions observed in oxygen-deficient perovskites and brownmillerites.<sup>39</sup>

The B-site-substituted Aurivillius phases,  $\text{Bi}_2\text{CaNb}_{2-y}\text{Ti}_y\text{O}_{9-y/2}$ , showed a significant change in the conductivity even for  $y = 0.1$  and 0.15. In the case of  $\text{Bi}_2\text{CaNb}_{1.9}\text{Ti}_{0.1}\text{O}_{8.95}$ , the activation energy for conduction decreases from 1.7 to 1.0 eV and the conductivity ( $5 \times 10^{-4}$  S/cm at 900 °C) is 2 orders of magnitude higher than in  $\text{Bi}_2\text{CaNb}_2\text{O}_9$ . The authors suggest that the difference between the observed effects of A and B site substitutions could be the result of several factors, including the location of the oxygen vacancies and the association of the vacancies with the dopants.

Gopalakrishnan and co-workers examined the solid solution of  $\text{Bi}_2\text{W}_{1-x}\text{Cu}_x\text{O}_{6-\delta}$ <sup>61</sup> and reported that for  $x < 0.7$  the orthorhombic symmetry of the parent structure is preserved, while a tetragonal unit cell is observed for the composition  $0.7 \leq x \leq 0.8$ . They reported high oxide ion conductivity in these materials; however, a recent report by Vannier et al. questions the phase purity of the samples on which the measurements were performed.<sup>62</sup>

Thomas et al. investigated a four-layer modified Aurivillius phase,  $\text{Bi}_4\text{BaTi}_3\text{MO}_{14.5}$  ( $M = \text{Sc, In, and Ga}$ ).<sup>38,63</sup> Arrhenius plots of the conductivity exhibited a discontinuity over the temperature range 750–850 °C. DTA data for these materials showed an endothermic transition occurring at the same temperature at which the discontinuity was observed in the Arrhenius plots of the conductivity. This transition, as in the case of  $\text{Bi}_2\text{Na}_x\text{Ca}_{1-x}\text{Nb}_2\text{O}_{9-x/2}$  and  $\text{Bi}_2\text{CaNb}_{2-y}\text{Ti}_y\text{O}_{9-y/2}$ , was attributed to an order/disorder transition of the oxygen vacancies. Figure 6 contains the superimposed conductivity and DTA data for  $\text{Bi}_4\text{BaTi}_3\text{GaO}_{14.5}$ , demonstrating the closeness between the temperatures of the discontinuity and the endothermic transition. Conductivities

at 900 °C for this system were  $2.5 \times 10^{-2}$ ,  $4.9 \times 10^{-2}$ , and  $4.5 \times 10^{-2}$  S/cm for  $\text{Bi}_4\text{BaTi}_3\text{ScO}_{14.5}$ ,  $\text{Bi}_4\text{BaTi}_3\text{InO}_{14.5}$ , and  $\text{Bi}_4\text{BaTi}_3\text{GaO}_{14.5}$ , respectively.

Kendall et al. examined the ionic conductivity in the three-layer Aurivillius system,  $\text{Bi}_2\text{Sr}_2\text{B}'_2\text{B}''\text{O}_{11.5}$ , [ $\text{B}' = \text{Nb, Ta}$ ;  $\text{B}'' = \text{Al, Ga}$ ],<sup>64–66</sup> where aliovalent cation substitutions were carried out on the B site. On the basis of powder X-ray diffraction and TEM data, the oxygen-deficient materials were indexed to a tetragonal unit cell (e.g.,  $a = 3.91$  Å,  $c = 33.3$  Å for  $\text{Bi}_2\text{Sr}_2\text{Nb}_2\text{AlO}_{11.5}$ ) with lattice constants in agreement with the non-oxygen-deficient three-layer structures,  $\text{Bi}_2\text{Sr}_2\text{B}'_2\text{TiO}_{12}$ , ( $\text{B}' = \text{Nb, Ta}$ ) (e.g.,  $a = 3.89$  Å,  $c = 33.18$  Å for  $\text{Bi}_2\text{Sr}_2\text{Nb}_2\text{TiO}_{12}$ ).<sup>64</sup> Conductivity data, along with EMF and oxygen partial pressure dependency measurements, indicated that these materials were ionic conductors with conductivities of  $10^{-2}$  S/cm at 800 °C. In the case of  $\text{Bi}_2\text{Sr}_2\text{Nb}_2\text{GaO}_{11.5}$ , the conductivity was predominately ionic above an oxygen partial pressure of  $10^{-5}$  atm, whereupon n-type electronic conduction was observed. For  $\text{Bi}_2\text{Sr}_2\text{Ta}_2\text{GaO}_{11.5}$ , ionic conductivity was maintained to a partial pressure of  $10^{-10}$  atm oxygen; at  $p(\text{O}_2)$  less than  $10^{-10}$  atm the compound decomposed. The conductivities were several orders of magnitude higher than those measured for the structurally-related non-oxygen-deficient phases,  $\text{Bi}_2\text{Sr}_2\text{B}'_2\text{TiO}_{12}$  ( $\text{B}' = \text{Nb, Ta}$ ). On the basis of oxygen partial pressure measurements, the non-oxygen-deficient phases were classified as n-type electronic conductors.

Similar to the Aurivillius phases discussed previously, the conductivity data for these three-layer systems indicated that these materials underwent order/disorder transitions between 700 and 800 °C. DTA data of the oxygen deficient materials displayed endothermic transitions at temperatures similar to those at which discontinuities were observed in the Arrhenius plots of the conductivity. Upon cooling, the samples exhibited extreme hysteresis in their conductivities (see Figure 5).

**Intrinsic Vacancies.** The most conductive Aurivillius phase reported to date is  $\text{Bi}_2\text{VO}_{5.5}$ . As a result, much research has focused on understanding both doped and undoped  $\text{Bi}_2\text{VO}_{5.5}$ . In 1988, Abraham et al. first reported the oxide ion conductivity in  $\text{Bi}_2\text{VO}_{5.5}$ .<sup>43</sup> Three conductivity regimes were observed, corresponding to the  $\alpha$ ,  $\beta$ , and  $\gamma$  phases. Although all three phases show significant oxide ion conductivity, the high-temperature  $\gamma$ -phase exhibits an extremely low activation energy (0.17 eV), a conductivity of over  $10^{-1}$  S/cm at 600 °C, and a transference number,  $t_i$ , close to unity in air. In measuring the conductivity of single crystals of  $\text{Bi}_2\text{VO}_{5.5}$ , it was observed that the conductivity in the crystallographic  $ab$  plane was several orders of magnitude higher than along the  $c$  direction.<sup>67</sup> This is consistent with the oxygen-deficient perovskite layers being responsible for the oxide ion conduction.<sup>55</sup> The magnitude of the conductivity for sintered powders was closest to

(61) Sharma, V.; Shukla, A. K.; Gopalakrishnan, J. *J. Mater. Chem.* **1994**, *4*, 703.

(62) Vannier, R. N.; Nowogrocki, G.; Mairesse, G. *J. Mater. Chem.* **1995**, *5*, 361.

(63) Thomas, J. K.; Kendall, K. R.; Zur Loye, H.-C. *Solid State Ionics* **1994**, *70/71*, 225.

(64) Kendall, K. R.; Thomas, J. K.; zur Loye, H. C. *Chem. Mater.* **1995**, *7*, 50.

(65) Kendall, K. R.; Navas, C.; zur Loye, H.-C. In *Materials Research Society Symposium Proceedings: Solid State Ionics IV*; Nazri, G.-A., Tarascon, J.-M., Schreiber, M., Eds.; MRS: Boston, MA, 1995; Vol. 369, p 355.

(66) Kendall, K. R.; Thomas, J. K.; zur Loye, H.-C. *Solid State Ionics* **1994**, *70/71*, 221.

(67) Mairesse, G., In *Fast Ion Transport In Solids*, Scrosati, B., Ed.; Kluwer Academic Publishers: New York, 1993; p 271.

the single crystal conductivity parallel to the *ab* plane.

The low-temperature conductivity behavior of  $\text{Bi}_2\text{VO}_{5.5}$  is enhanced by dopants in the BIMEVOX family which help to stabilize the  $\gamma$ -phase. The copper member was the first to be synthesized and remains one of the best conducting in the family.<sup>52</sup> The conductivity of  $\text{Bi}_2\text{V}_{0.9}\text{Cu}_{0.1}\text{O}_{5.35}$  at 250 °C,  $10^{-3}$  S/cm, is about 2 orders of magnitude higher than that of the undoped  $\text{Bi}_2\text{VO}_{5.5}$  at 250 °C. Dygas et al. carried out impedance studies and observed a change in the slope of the Arrhenius plot of the total conductivity between 452 and 477 °C,<sup>68</sup> resulting in a decrease in the activation energy from 0.666(3) to 0.486(9) eV. The change in slope is a residual of the structural transition from the  $\beta$ -phase to the  $\gamma$ -phase observed in the undoped phase. In oxygen pressure dependence studies, Iharada et al. observed a nonlinear dependence below oxygen partial pressures of  $10^{-2}$  atm, indicating an electronic contribution to the total conductivity.<sup>69</sup>

Chadwick and Francklin, in an extension of their examination of the ionic conduction in  $\text{Bi}_2\text{O}_3$ , looked at the conductivity and thermoelectric power of  $\text{Bi}_2\text{VO}_{5.5}$  and BICUVOX.<sup>50,70</sup> In comparison with  $\text{Bi}_2\text{O}_3$ , the conduction process in the bismuth vanadium systems was much more complicated, and it could not be explained by a simple vacancy-hopping model. In fact, they were not able to elucidate the exact mechanism for the conduction. Both the conductivity and the thermoelectric power were measured as a function of oxygen partial pressure. At moderate temperatures,  $\text{O}^{2-}$  was the predominant charge carrier; however, at higher temperatures and lower  $p(\text{O}_2)$ , the evidence was more ambiguous. The  $p(\text{O}_2)$  dependence of the conductivity along with the thermoelectric power data indicated that although ionic conductivity dominated down to  $10^{-6}$  atm  $\text{O}_2$ , there was electronic conduction present. The authors suggest that changes occur in the oxidation states of the dopants at the surface, an effect which is more evident in the thermoelectric power data than in the conductivity data.

Goodenough et al. examined the  $p(\text{O}_2)$  dependence of the conductivity for some BIMEVOX systems, especially BICUVOX.<sup>71</sup> At temperatures greater than 400 °C, the conductivity for  $\text{Bi}_2\text{V}_{0.9}\text{Cu}_{0.1}\text{O}_{5.2}$  increased under both reducing and oxidizing conditions, leading to the conclusion that there is some electronic contribution to the total conductivity.

Electrochemical measurements, including redox stability, impedance spectroscopy, and potentiometric measurements, were carried out by Iharada et al. on BIMEVOX (ME = Cu, Ni).<sup>69</sup> Both materials display transference numbers close to one,  $t_i = 0.987$ , at 557 °C; however, some electronic conduction is observed when the current through the material is increased from 1 to 4.6 mA. Measurements of the conductivity as a function of oxygen partial pressure for both BINIVOX and BICUVOX revealed small changes in the conductivity for oxygen partial pressures ranging from 1 to  $10^{-4}$

H																		He
Li	Be												B	C	N	O	F	Ne
Na	Mg												Al	Si	P	S	Cl	Ar
K	Ca	Sc	Ti	V	Cr	Mn	Fe	Co	Ni	Cu	Zn	Ga	Ge	As	Se	Br	Kr	
Rb	Sr	Y	Zr	Nb	Mo	Tc	Ru	Rh	Pd	Ag	Cd	In	Sn	Sb	Te	I	Xe	
Cs	Ba	La	Hf	Ta	W	Re	Os	Ir	Pt	Au	Hg	Tl	Pb	Bi	Po	At	Rn	

Figure 7. Elements examined as possible dopants in  $\text{Bi}_2\text{VO}_{5.5}$  structure.

atm ( $\approx 2\%$  at 200 °C and  $\approx 4\%$  at 650 °C). Because of the similarities between the copper- and nickel-doped systems, it is believed that the electronic characteristics of these materials are dominated by the vanadium and the bismuth and not by the dopant.

With an eye to possible applications, Krok et al. studied the effects of preparation conditions on the physical properties of BICUVOX,<sup>72</sup> while Reiselhuber et al. examined grain size effects on conductivity.<sup>73</sup> While preparation conditions did affect the conductivity, they did so to a lesser degree than is the case for other oxide conductors, such as  $\text{ZrO}_2$ . Similar studies have also been carried out by several groups on BICOVOX.<sup>74,75</sup> Overall, the best conductivities for BICUVOX and BICOVOX were observed for samples that were sintered at 800 °C.

Because of the high conductivity first reported for BICUVOX, many different cations have subsequently been substituted for the vanadium. Mairesse has summarized results for the substitutions of various metal cations in the vanadium site.<sup>67</sup> Figure 7 shows the wide range of cations explored, including antimony,<sup>51</sup> nickel,<sup>55</sup> molybdenum,<sup>76</sup> germanium,<sup>77</sup> titanium,<sup>71</sup> and niobium.<sup>71</sup> Both BITIVOX and BINBVOX have reported conductivities nearly equal that of BICUVOX,<sup>56</sup> whereas the performance of other BIMEVOX compounds result in lower oxide ion conductivities, though still significantly higher than in undoped  $\text{Bi}_2\text{VO}_{5.5}$ .

A number of double substitutions for vanadium were attempted by Vannier et al.<sup>36</sup> Combinations such as Cu/Ni, Cu/Zn, Ni/Zn, and Cu/Mo were synthesized and their conductivities studied. However, no improvement in the conductivity was found with respect to the Cu-substituted  $\text{Bi}_2\text{VO}_{5.5}$ .

Substitution for the Bi in the bismuth oxide plane has been studied to determine the effect of the  $\text{Bi}_2\text{O}_2^{2+}$  layer on the conductivity. As mentioned earlier, several atoms can be substituted for the bismuth, including lead and antimony. Vannier et al. looked at the solid solution of  $\text{Bi}_{2-y}\text{Pb}_y\text{VO}_{5.5-0.5y}$  for  $0.0 \leq y \leq 0.20$  and found no evidence for stabilization of the  $\gamma$ -phase.<sup>78</sup> The substitution of lead on the bismuth site did not improve the conductivity relative to  $\alpha$ - $\text{Bi}_2\text{VO}_{5.5}$ . Single crystals

(72) Krok, F.; Bogusz, P.; Wasiucionek, M.; Jakubowski, W.; Dygas, J. *Mater. Sci. Eng. B—Solid State Mater.* **1993**, *21*, 70.

(73) Reiselhuber, K.; Dorner, G.; Breiter, M. W. *Electrochim. Acta* **1993**, *38*, 969.

(74) Krok, F.; Bogusz, W.; Jakubowski, W.; Dygas, J. R.; Bangobango, D. *Solid State Ionics* **1994**, *70/71*, 211.

(75) Essalim, R.; Tanouti, B.; Bonnet, J.-P.; Reau, J. M. *Mater. Lett.* **1992**, *13*, 382–386.

(76) Vannier, R. N.; Mairesse, G.; Abraham, F.; Nowogrocki, G. *J. Solid State Chem.* **1993**, *103*, 441.

(77) Lee, C. K.; Tan, M. P.; West, A. R. *J. Mater. Chem.* **1994**, *4*, 525.

(78) Vannier, R. N.; Mairesse, G.; Nowogrocki, G.; Abraham, F.; Boivin, J. C. *Solid State Ionics* **1992**, *53–56*, 713.

(68) Dygas, J. R.; Krok, F.; Bogusz, W.; Kurek, P.; Reiselhuber, K.; Breiter, M. W. *Solid State Ionics* **1994**, *70/71*, 239.

(69) Iharada, T.; Hammouche, A.; Fouletier, J.; Kleitz, M.; Boivin, J. C.; Mairesse, G. *Solid State Ionics* **1991**, *48*, 257.

(70) Chadwick, A. V.; Francklin, A. J. *Philos. Mag. A* **1993**, *68*, 787.

(71) Goodenough, J. B.; Manthiram, A.; Paranthaman, P.; Zhen, Y. S. *Solid State Ionics* **1992**, *52*, 105.



were obtained for a double substitution by Pb for both bismuth and vanadium,  $(\text{Bi}_{1.9}\text{Pb}_{0.1})(\text{Pb}_{0.1}\text{V}_{0.9})\text{O}_{11-\delta}$ . EDS data (metal composition of  $\text{Bi}_{1.9}\text{Pb}_{0.2}\text{V}_{0.9}$ ) and single-crystal structural refinement were consistent with substitution on both the bismuth and vanadium sites. The conductivity in the lead double substitution was almost as high as that for the BICUVOX system.<sup>78</sup> Concentration cell measurements indicated that the transference number,  $t_i$ , for the lead double substitution was between 0.90 and 0.95.

### Future Directions

Materials based upon Aurivillius phases represent a new class of oxide ion conductors. Ultimately, however, they will prove useful only if their properties can be successfully applied to current applications. For example, solid oxide fuel cells (SOFCs), which have been the "technology of tomorrow" for several decades, not only require a solid electrolyte with excellent ionic conductivity but also require an electrolyte that meets numerous other design criteria (e.g., compatible thermal expansion coefficients, lattice match, etc.). One important characteristic of stabilized zirconia is the low electronic conductivity that is present under both oxidizing and reducing conditions. Aurivillius phases, although exhibiting excellent ionic conductivity, have significant problems with electronic conduction at low partial pressures of oxygen. Increasing the number of perovskite layers from  $n = 1$  to 4 does increase the reduction stability; albeit, this is at the detriment to the overall magnitude of the ionic conductivity.<sup>79</sup>

The presence of electronic conductivity in Aurivillius-based oxide ion conductors under reducing atmospheres, although problematic for use in SOFCs, is in fact beneficial for some commercial applications. Both partial oxidation catalysis and oxygen separation require some level of mixed ionic/electronic conduction. The fact that electronic conduction exists in  $\text{Bi}_2\text{VO}_{5.5}$  makes it an attractive candidate for use in these applications. Cherrak et al. examined the oxidative coupling of methane (OCM) using  $\text{Bi}_2\text{VO}_{5.5}$  and BIMEVOX (Cu, Fe, and Sr) as catalysts.<sup>5</sup> An increased methane conversion rate was correlated with an increase in the oxygen vacancy concentration, as expected for a reaction of this type.<sup>80</sup> In addition, the BIMEVOX systems showed an improved  $\text{C}_2$  selectivity as compared to  $\text{Bi}_2\text{VO}_{5.5}$ . However, neither the catalytic activity nor

the selectivity represent a significant improvement over existing OCM catalysts.

Although Cherrak and co-workers used standard solid-state techniques to synthesize  $\text{Bi}_2\text{VO}_{5.5}$  and BIMEVOX as a powder, alternative synthetic methods need to be developed to realize the full potential of these materials. Specifically, many applications would require thin films or high surface area powders and some research has been reported with regard to both. Pell et al. have synthesized both powders and thin films of  $\text{Bi}_2\text{VO}_{5.5}$  and BIMEVOX using a sol-gel route,<sup>81</sup> while Bhattacharya et al. used a bismuth nitrate hydrate and ammonium metavanadate coprecipitation technique to produce fully crystalline  $\text{Bi}_2\text{VO}_{5.5}$  at 320 °C.<sup>82</sup> Additional experimentation is required to further develop techniques for obtaining Aurivillius phases in the desired form.

### Conclusion

Work on Aurivillius phases, with both intrinsic and extrinsic oxygen vacancies, has resulted in materials that exhibit a wide range of properties. The most successful oxide ion conductors are the metal-doped bismuth vanadium oxides,  $\text{Bi}_2\text{M}_x\text{V}_{1-x}\text{O}_\delta$ , which have the highest reported oxide ion conductivity of any solid electrolyte at low temperatures. Applications that exploit this conductivity will require synthetic techniques that result in high surface area powders, thin films, or ceramic green bodies. Aurivillius phases with extrinsic vacancies, although exhibiting much lower conductivity than BIMEVOX, are much more amenable to structural and compositional manipulation. The ability to modify these systems, and thereby to exert control over their conductive behavior, suggests that despite the less than desired performance to date, further research should be pursued.

**Acknowledgment.** The authors would like to thank the National Science Foundation for financial support through Grant DMR-9200688. K.R.K. acknowledges an NSF training grant (CHE-9256458) in environmental chemistry.

CM9503083

(79) Thomas, J. K. Thesis, Massachusetts Institute of Technology, 1994.

(80) Sleight, A. W. In *Advanced Materials in Catalysis*, Burton, J. J., Garten, R. L., Ed.; Academic Press: New York, 1977; p 181.

(81) Pell, J. W., Ying, J. Y., zur Loye, H.-C. *Mater. Lett.* **1995**, *25*, 157.

(82) Bhattacharya, A. K.; Mallick, K. K. *Solid State Commun.* **1994**, *91*, 357.

(83) van Herle, J.; A. J., M.; Thampi, K. R. *J. Mater. Sci.* **1994**, *29*, 3691.

(84) Takahashi, T.; Iwahara, H.; Arao, T. *J. Appl. Electrochem.* **1975**, *5*, 187.

(85) Moon, P. K. Ph.D. Thesis, MIT, 1980.

(86) Sharma, V.; Shukla, A. K.; Gopalakrishnan, J. *Solid State Ionics* **1992**, *58*, 359.